The Journal of Immunology

RESEARCH ARTICLE | AUGUST 15 2016

Netrin-1 Augments Chemokinesis in CD4+ T Cells In Vitro and Elicits a Proinflammatory Response In Vivo FREE

Leo Boneschansker; ... et. al

J Immunol (2016) 197 (4): 1389–1398.
https://doi.org/10.4049/jimmunol.1502432

Netrin-1 Augments Chemokinesis in CD4$^+$ T Cells In Vitro and Elicits a Proinflammatory Response In Vivo

Leo Boneschansker,*,†,‡ Hironao Nakayama,§ Michele Eisenga,* Johannes Wedel,*,† Michael Klagsbrun,§ Daniel Irimia,‡ and David M. Briscoe*,†

Netrin-1 is a neuronal guidance cue that regulates cellular activation, migration, and cytoskeleton rearrangement in multiple cell types. It is a chemotropic protein that is expressed within tissues and elicits both attractive and repulsive migratory responses. Netrin-1 has recently been found to modulate the immune response via the inhibition of neutrophil and macrophage migration. However, the ability of Netrin-1 to interact with lymphocytes and its in-depth effects on leukocyte migration are poorly understood. In this study, we profiled the mRNA and protein expression of known Netrin-1 receptors on human CD4$^+$ T cells. Neogenin, uncoordinated-5 (UNC5)A, and UNC5B were expressed at low levels in unstimulated cells, but they increased following mitogen-dependent activation. By immunofluorescence, we observed a cytoplasmic staining pattern of neogenin and UNC5A/B that also increased following activation. Using a novel microfluidic assay, we found that Netrin-1 stimulated bidirectional migration and enhanced the size of migratory subpopulations of mitogen-activated CD4$^+$ T cells, but it had no demonstrable effects on the migration of purified CD4$^+$CD25$^+$CD127^{dim} T regulatory cells. Furthermore, using a short hairpin RNA knockdown approach, we observed that the promigratory effects of Netrin-1 on T effectors is dependent on its interactions with neogenin. In the humanized SCID mouse, local injection of Netrin-1 into skin enhanced inflammation and the number of neogenin-expressing CD3$^+$ T cell infiltrates. Neogenin was also observed on CD3$^+$ T cell infiltrates within human cardiac allograft biopsies with evidence of rejection. Collectively, our findings demonstrate that Netrin-1/neogenin interactions augment CD4$^+$ T cell chemokinesis and promote cellular infiltration in association with acute inflammation in vivo. ***The Journal of Immunology*****, 2016, 197: 1389–1398.**

Axonal guidance molecules belong to at least four families, namely netrins, semaphorins, slits, and ephrins, and they regulate cellular activation, migration, and cytoskeleton rearrangement in multiple cell types (1–3). An increasing number of reports indicate that guidance receptors are also expressed on leukocyte subsets where they primarily function to regulate migration (4–7). For instance, the binding of class 3 semaphorin family molecules to the neuropilin-1 receptor results in antimigration and cytoskeletal collapse in multiple cell types, including leukocytes (8–10). Slit–Robo interactions inhibit chemokine-induced leukocyte migration and protect against neutrophil-induced ischemia/reperfusion injury (6, 11, 12). Additionally, ephrins are reported to function in chronic inflammation by enhancing both T cell maturation and leukocyte trafficking, for instance in rheumatoid arthritis (13, 14).

Netrin-1 is a more recently described guidance cue with unique effects on the immune response (4, 15, 16). It is a major growth and promigratory chemotactic factor (17), and it has been reported to elicit chemoinhibitory responses in bulk populations of leukocytes (4, 15, 18). Netrin-1 is a secreted laminin-related protein that mediates signaling through seven receptors, namely members of the uncoordinated-5 (UNC) family (UNC5A–D), deleted in colorectal cancer (DCC) family, neogenin, and Down syndrome cell adhesion molecule (DSCAM) (19). The binding of Netrin-1 to the UNC5 family of receptors promotes axonal chemorepulsion, whereas its binding to neogenin and/or DCC promotes chemoattraction (19). Initial reports demonstrated that the UNC5 family of receptors are expressed at high levels on human peripheral blood leukocytes and that Netrin-1 inhibits migration toward chemotactic stimuli in vitro in Transwell assays (4). Additional reports indicate that it is anti-inflammatory in models of peritonitis (4, 18), acute lung injury (20), hypoxia-induced inflammation (21), acute colitis (22), as well as in kidney ischemia/reperfusion injury (15). In these and other studies, Netrin-1 was proposed to dominantly function via interactions with UNC5 family receptors (4, 15, 16, 20–22).

However, more recent studies suggest that the effects of Netrin-1 may be more complex (19, 23). For example, in an atherosclerosis model, Netrin-1 was found to retain macrophages within plaques by inhibiting macrophage emigration from the inflammatory site (5); additionally, Netrin-1 has been found to promote chronic inflammation in adipose tissue (24). Several studies have evaluated Netrin-1 receptor biology using neogenin knockout mice,

*Transplant Research Program, Division of Nephrology, Department of Medicine, Boston Children's Hospital, Boston, MA 02115; †Department of Pediatrics, Harvard Medical School, Boston, MA 02115; ‡Center for Engineering in Medicine, Department of Surgery, Massachusetts General Hospital, Harvard Medical School, Shriners Hospitals for Children, Boston, MA 02114; and §Vascular Biology Program, Department of Surgery, Boston Children's Hospital, Harvard Medical School, Boston, MA 02115

ORCIDs: 0000-0002-9371-2650 (H.N.); 0000-0002-2484-6233 (M.E.); 0000-0002-3490-8477 (J.W.); 0000-0001-7347-2082 (D.I.).

Received for publication November 17, 2015. Accepted for publication June 14, 2016.

This work was supported by National Institutes of Health Grants R01AI092305 and AI04675 (to D.M.B.) and GM092804 (to D.I.) and in part by funding from the Casey Lee Ball Foundation (to D.M.B.). L.B. was supported by National Institutes of Health Grants T32DK07726 and T32AI007529. All microfabrication was performed at the National Institute of Biomedical Imaging and Bioengineering–funded (Grant EB002503) BioMEMS Resource Center.

Address correspondence and reprint requests to Dr. David M. Briscoe, Transplant Research Program, Division of Nephrology, Boston Children's Hospital, 300 Longwood Avenue, Boston, MA 02115. E-mail address: david.briscoe@childrens.harvard.edu

The online version of this article contains supplemental material.

Abbreviations used in this article: Ct, threshold cycle; DCC, deleted in colorectal cancer; DP, directional persistence; DSCAM, Down syndrome cell adhesion molecule; hpf, high power field; huSCID, humanized SCID; shRNA, short hairpin RNA; Treg, T regulatory cell; UNC5, uncoordinated-5.

which mount a reduced inflammatory peritonitis reaction (25) and have less leukocyte infiltrates and reduced inflammation in models of acute lung injury (26) and ischemia/reperfusion injury (27).

These collective studies allow for the possibility that both chemoattractive/neogenin and chemorepulsive/UNC5 family receptors may be coexpressed on subsets of leukocytes and that the relative expression of the promigratory receptor neogenin may determine the ability of Netrin-1 to elicit a pro- versus anti-inflammatory response. However, little is known about Netrin-1/netrin receptor interactions in $CD4^+$ T cells and adaptive immunity. In these studies, we used a novel in vitro microfluidic assay to evaluate the effects of Netrin-1 on migration of $CD4^+$ T cells at the single-cell level. Our findings demonstrate that Netrin-1 induces bidirectional migratory responses, and that it increases the size of migratory subpopulations of mitogen-activated $CD4^+$ T cells. Furthermore, we observed that Netrin-1 primarily regulates T effector migration and does not alter the migration of purified populations of $CD4^+CD25^+CD127^{dim}$ T regulatory cells (Tregs). Additionally, we find that these biological effects of Netrin-1 on $CD4^+$ T cell migration are dependent on the expression of neogenin. In vivo, the administration of Netrin-1 into human skin in the humanized SCID (huSCID) mouse augmented the recruitment of $CD3^+$ T cells and the local inflammatory response. We also observed high levels of neogenin expression on $CD3^+$ T cell infiltrates within inflamed skin from the huSCID mice and within endomyocardial biopsies from human cardiac transplant recipients, suggesting that it is of great pathophysiological significance. Taken together, our findings indicate that the primary function of Netrin-1 is to augment chemokinesis of activated $CD4^+$ T effector cells. Furthermore, we show that this function of Netrin-1 is elicited via interactions with neogenin. Our findings are most suggestive that Netrin-1/neogenin interactions function to augment T cell recruitment into sites of acute inflammation, including allografts undergoing rejection.

Materials and Methods

Reagents

Anti-human UNC5A and anti-neogenin Abs were purchased from Santa Cruz Biotechnology (Dallas, TX), anti-UNC5B or anti-DCC was from Abcam (Cambridge, MA), and anti-CD3 Ab was from Dako (Carpinteria, CA). Goat anti-mouse Alexa Fluor 488 and goat anti-rabbit Alexa Fluor 594 were purchased from Life Technologies (Carlsbad, CA). Human Netrin-1 was produced as previously described (23). Briefly, 293T cells were transfected with Netrin-1/pcDNA3.1/V5-His-TOPO plasmid using FuGENE HD transfection reagent (Roche Applied Science, Indianapolis, IN), and secreted Netrin-1 was purified from the culture medium using HiTrap HP chelating columns (GE Healthcare Bio-Sciences, Pittsburgh, PA), as described (28). Anti-human CD3 and anti-human CD28 were purchased from BD Pharmingen (San Jose, CA), and PHA was from Fisher Scientific (Pittsburgh, PA).

$CD4^+$ T lymphocyte culture

Human blood samples were obtained from consenting healthy volunteers in accordance with Institutional Review Board approval by Boston Children's Hospital. PBMCs were harvested by gradient centrifugation (2200 rpm for 30 min) using Ficoll (GE Healthcare, Waukesha, WI), and $CD4^+$ T cells were positively isolated from the PBMCs using magnetic beads (Dynabeads $CD4^+$ isolation kit; Invitrogen, Carlsbad, CA) according to the manufacturers' protocols. $CD4^+CD25^+$ and $CD4^+CD25^-$ T lymphocytes were isolated by positive selection, and the $CD127^{dim}$ subset of $CD4^+CD25^+$ Tregs were isolated by a subsequent negative selection using the human $CD4^+CD127^{lo}CD25^+$ Treg isolation kit (Stemcell Technologies, Vancouver, BC, Canada) according to the manufacturer's protocol. $CD4^+$ T lymphocyte subsets were cultured in RPMI 1640 media (Cambrex, Charles City, IA) containing 10% FBS, 2 mM L-glutamine, 100 U ml^{-1} penicillin/streptomycin (Life Technologies-Invitrogen), 1% sodium bicarbonate, and 1% sodium pyruvate (Cambrex). $CD4^+$ T cells were used immediately or following a freeze thaw (occasionally) and were activated with anti-human CD3 and anti-human CD28 (each at 1 μg/ml) or PHA (2.5 μg/ml) for intervals of 6–48 h. $CD4^+CD25^-$ T cells were cultured in medium (above) and stimulated with 1 μg/ml plate-bound anti-CD3 Ab in the absence or presence of different concentrations of Netrin-1 (0.1–1 μg/ml).

Real-time PCR

Total RNA was isolated from $CD4^+$ T cells following mitogen activation using the RNeasy isolation kit (Qiagen, Valencia, CA). cDNA was generated using qScript Supermix (Quanta Biosciences, Gaitherburg, MD), according to the manufacturer's instructions. The quantitative RT-PCR primers used in the present study are as follows: UNC5A, forward 5′-TCTACCTCACGCTGCACAAG-3′ and reverse 5′-AGTGGTCCATAGCCAGGATG-3′; UNC5B, forward 5′-TCCAGCTGCATACCACTCTG-3′ and reverse 5′-GGATGGACAGTGGGATCTTG-3′; UNC5C, forward 5′-AGCAAGGCAGACTGATCCAT-3′ and reverse 5′-TCAGCAAGCTGACTCCTGAA-3′; UNC5D, forward 5′-AGTGGGTCCATCAGAACGAG-3′ and reverse 5′-CATGGAAGTCCTCCACCTGT-3′; neogenin, forward 5′-GTGTTGCCATGTGTTGCTTC-3′ and reverse 5′-ACCTGCCAGCAATACCAATC-3′; DCC, forward 5′-AGGTCGTCATGGAGATGGAG-3′ and reverse 5′-TCACAAGCAGGTTGCTGTTC-3′; DSCAM, forward 5′-CGAATGCACATCGACATACC-3′ and reverse 5′-TCAGCATCCGTCAACAGAAC-3′; GAPDH, forward 5′-ACCACAGTCCATGCCATCAC-3′ and reverse 5′-TCCACCACCCTGTTGCTGTA-3′; IFN-γ, forward 5′-TCGGTAACTGACTTGAATGTCCA-3′ and reverse 5′-TCGCTTCCCTGTTTTAGCTGC-3′; IL-2, forward 5′-AACTCCTGTCTTGCATTGCAC-3′ and reverse 5′-GCTCCAGTTGTAGCTGTGTTT-3′; IL-4, forward 5′-CCAACTGCTTCCCCCTCTG-3′ and reverse 5′-TCTGTTACGGTCAACTCGGTG-3′; IL-5, forward 5′-TCTACTCATCGAACTCTGCTGA-3′ and reverse 5′-CCCTTGCACAGTTTGACTCTC-3′; IL-6, forward 5′-ACTCACCTCTTCAGAACGAATTG-3′ and reverse 5′-CCATCTTTGGAAGGTTCAGGTTG-3′; IL-10, forward 5′-TCAAGGCGCATGTGAACTCC-3′ and reverse 5′-GATGTCAAACTCACTCATGGCT-3′; IL-17A, forward 5′-AGATTACTACAACCGATCCACCT-3′ and reverse 5′-GGGGACAGAGTTCATGTGGTA-3′; β2-microglobulin, forward 5′-TTTCATCCATCCGACATTGA-3′ and reverse 5′-CCTCCATGATGCTGCTTACA-3′. Primers and cDNA were mixed with SYBR Green supermix (Quanta Biosciences) and real-time PCR was performed using the 7300 real-time PCR system (Applied Biosystems, Foster City, CA). A comparative threshold cycle (Ct) value was normalized for each sample using the formula: $\Delta Ct = Ct$ (gene of interest) − Ct (GAPDH or β2-micoglobulin). The relative expression was then calculated according to the $2^{-\Delta Ct}$ method.

Western blot analysis

Cells were lysed with radioimmunoprecipitation assay buffer (Boston Bioproducts, Boston, MA), and protease and phosphatase inhibitors (Thermo Scientific, Rockford, IL) were added. Proteins were separated on a Mini-Protean TGX precast gel (Bio-Rad Laboratories, Hercules, CA) and transferred onto a polyvinylidene difluoride membrane (Millipore, Billerica, MA). Membranes were blocked with 4% skimmed milk in TBS and 0.1% Tween 20 for 1 h and incubated with primary Abs (as indicated) overnight at 4°C. Membranes were subsequently washed and incubated with a species-specific secondary peroxidase-linked Ab for 90 min at room temperature, and the protein of interest was detected by chemiluminescence (Thermo Scientific, Tewksbury, MA).

Flow cytometry

$CD4^+$ T lymphocytes were stained with unconjugated anti-neogenin or a rabbit IgG isotype Ab (GeneTex, Irvine, CA) as a control for 30 min at 4°C. Cells were subsequently washed and incubated with species-specific secondary FITC-conjugated Ab for 30 min at 4°C. Data were acquired on a FACSCalibur (BD Biosciences) and analyzed using FlowJo software (Tree Star, Ashland, OR).

Cellular immunofluorescence

Unactivated and 48-h mitogen-activated (PHA 2.5 μg/ml) cells were plated onto ImmunoSelect adhesion slides (MoBiTec, Duesseldorf, Germany), washed, and blocked with 5% BSA (Fisher Scientific, Pittsburgh, PA) in PBS. The cells were subsequently incubated with primary Abs or a rabbit IgG isotype control Ab for 60 min at room temperature. After washing in PBS, cells were incubated with secondary Ab for 1 h. Finally, cells were mounted with ProLong Gold antifade with DAPI (Life Technologies), and staining was evaluated by microscopy using a Nikon Eclipse 80i microscope and a Retiga-2000R CCD camera (QImaging, Surrey, BC, Canada). Each image was collected and processed using NIS Elements (version 3.2) software. Images were analyzed using ImageJ (National Institutes of Health).

Short hairpin RNA knockdown

Lentivirus was produced with 293T cells, using the pPACKH1 HIV lentivector packaging kit and PureFection (System Biosciences, Mountain View, CA), together with neogenin short hairpin RNA (shRNA) plasmids (Neo1 Mission shRNA plasmids: shNeo-1 [TRCN0000311710] and shNeo-2 [TRCN0000118046]) or a control shRNA (Mission pLKO.1-puro non-target shRNA, Sigma-Aldrich, St. Louis, MO), according to the manufacturers' protocols. In all experiments, $CD4^+$ T cells were activated for 48 h (with anti-CD3/CD28) and simultaneously transfected with lentivirus containing Neo-shRNA or control shRNA. Cells were infected with shControl or shNEO1 lentivirus using a multiplicity of infection from 10 to 15.

Migration experiments

Migration of $CD4^+$ T cell subsets was analyzed in microfluidic devices designed for the analysis of live-time bidirectional migration patterns, as described previously (12). Briefly, three layers (3, 10, and 50 μm thick) of negative photoresist (SU8, Microchem, Newton, MA) were patterned on a silicon wafer by sequentially employing three photolithography masks and processing cycles, according to the manufacturer's instructions. The wafer with patterned photoresist was used as a mold to produce polydimethylsiloxane (Fisher Scientific, Fair Lawn, NJ) parts, which were subsequently bonded irreversibly to standard glass slides (75 × 25 mm; Fisher Scientific). The microfluidic devices were primed with chemoregulatory proteins 30 min prior to loading of the device with T cells. Netrin-1 and/or RANTES/CCL5 (BioLegend, San Diego, CA) were instilled into the device (~20 μl) in combination with 100 nM human fibronectin (Sigma-Aldrich) in cell culture media. After 15 min the solution was washed out of the device using complete media. Passive diffusion of chemoregulatory proteins from the reservoirs into the main channel creates a gradient from the reservoir (highest concentration) to the buffer channel (lowest concentration). Subsequently, 2×10^5 cells were gently delivered into the cell-loading chamber, where the cells were evenly distributed in the cell loading traps, from where they can migrate into 10-μm-wide migration channels. Cell migration is recorded using time-lapse imaging on a fully automated Nikon TiE microscope (×10 magnification) with biochamber heated to 37°C with 5% CO_2 gas for 8 h. Cell displacement was tracked manually using ImageJ (National Institutes of Health).

Analysis of cell migration

Cell migration inside migration channels was analyzed, as previously described (12), using four parameters: 1) the percentage of migrating cells, 2) the direction of migration, 3) the speed of migration, and 4) the directional persistence (DP) following migration. The percentage of migrating cells was evaluated as the number of cells migrating in each direction as a ratio of the total number of cells loaded in the cell reservoir. The direction of migration was evaluated as a response either toward or away from the chemokine. Speed was calculated by the total distance traveled divided by the duration of migration, and DP was determined by comparing the relative displacement of cells from their initial to their final position within the migration channel as a ratio of the total distance traveled during an 8-h time period. Cells migrating persistently toward the chemokine reservoir without changing direction were determined to have a DP equal to "1," and cells migrating persistently away from the gradient have a DP equal to "−1." DP values <1 identify cells that change direction in the course of migration. For instance, a DP value of 0 reflects cells that migrate back and forth through the migration channels and ultimately return to their initial starting position by the end of the experiment.

Humanized SCID mouse model

Human neonatal foreskins were obtained from the birthing unit at the Brigham and Women's Hospital in accordance with Institutional Review Board approval. The skin was prepared under sterile conditions and was transplanted onto SCID mice. Once healed (after ~6 wk), the mice were humanized by i.p. injection of 3×10^8 human PBMCs. At days 0 and 7 following humanization, growth factor reduced Matrigel (BD Biosciences, Bedford, MA) combined with Netrin-1 (5 μg diluted in sterile PBS) was injected intradermally into the skin graft. Injection of Matrigel with PBS served as a control. After 14 d, the mice were euthanized and the skin grafts were harvested for evaluation by histology. Each skin was divided into two parts, one of which was frozen in liquid N_2/OCT compound (Sakura Finetek, Torrance, CA) for later cryosectioning and histochemistry; the other part was fixed in formalin and embedded in paraffin, for processing with H&E staining.

Immunohistochemistry/immunofluorescence

Skin grafts were cut into 4-μm cryosections and were initially blocked with 0.3% hydrogen peroxide or 10% serum (host of secondary Ab) in 0.05% Tris/Tween, washed, and incubated with the primary Ab for 1 h. Control sections were incubated with a species-specific IgG. After washing in PBS, sections were incubated with a secondary species-specific HRP-conjugated or fluorescent-tagged Ab for 1 h. For immunohistochemistry, staining was resolved using amino-ethylcarbazole, and the slides were mounted in glycerol gelatin (Sigma-Aldrich); for immunofluorescence, the sections were mounted with VectorShield mounting medium with DAPI (Vector Laboratories, Burlingame, CA).

Human endomyocardial biopsies were collected from cardiac transplant recipients during routine posttransplantation care and were stored at −80°C until use in this study. Collection was approved by the Human Research Committee, Brigham and Women's Hospital (Boston, MA). Research studies were performed after clinicopathologic diagnoses and clinical care was completed. Four-micrometer cryosections were prepared as described above and stained with anti-human CD3 and anti-human neogenin, as above. Staining of skin and heart was evaluated by microscopy using a Nikon Eclipse 80i microscope and a Retiga-2000R CCD camera (QImaging). Confocal microscopy imaging was performed using a Leica TCS SP5 X laser scanning microscope (Leica, Mannheim, Germany).

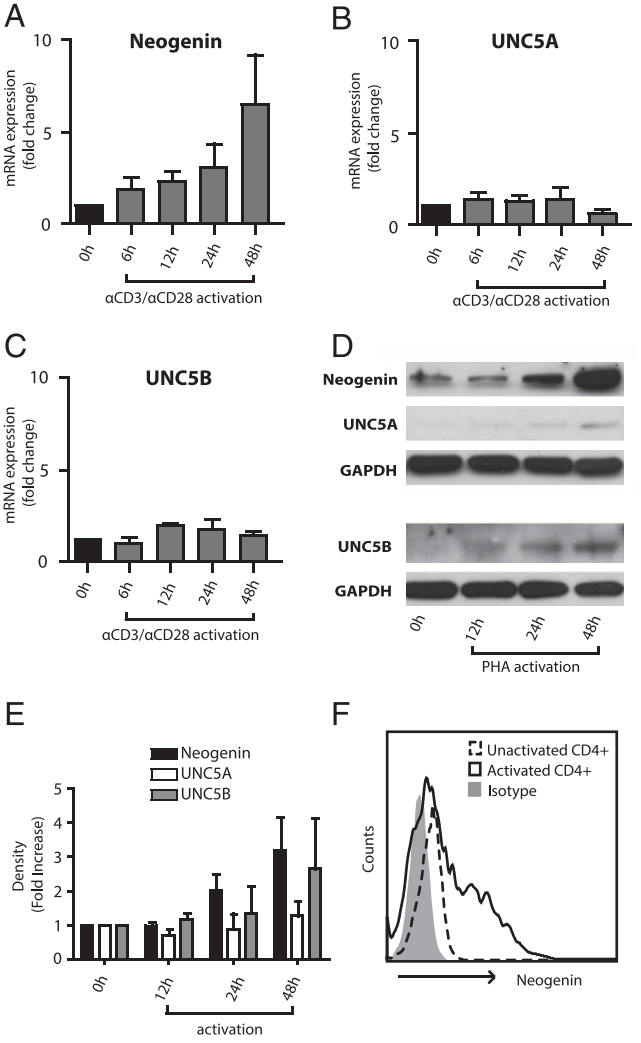

FIGURE 1. Netrin-1 receptor expression by human $CD4^+$ T lymphocytes. The expression of known Netrin-1 receptors was analyzed at the mRNA level by quantitative PCR (**A**–**C**), at the protein level by Western blot analysis (**D** and **E**), and by FACS after 48 h of activation (**F**). (A–C) Mean fold change in mRNA expression ± SEM. In (D), induced expression of neogenin, UNC5A, and UNC5B is illustrated, and (E) illustrates densitometric analysis of $n = 3$ independent Western blots. The illustrated data in (A)–(F) are representative of $n = 3$ independent experiments.

Statistical analysis

Statistical significance was determined using the Student *t* test or one-way ANOVA for normally distributed data and the Mann–Whitney *U* test for data that did not have normal distribution. Differences were considered statistically significant when p values were <0.05.

Results

Neogenin is the dominant Netrin-1 receptor expressed by activated CD4+ T lymphocytes

Purified human CD4+ T cells were initially profiled at the mRNA level for known Netrin-1 receptors. Using quantitative PCR, we found neogenin, UNC5A, and UNC5B, and low levels of DCC on unactivated cells (Fig. 1A–C, Supplemental Fig. 1A); in contrast, UNC5C-D and DSCAM were not expressed at any significant level (data not shown). Following mitogenic activation with anti-CD3/anti-CD28, there was a marked time-dependent increase in the expression of neogenin during 6–48 h (average 7-fold, Fig. 1A) and a smaller increase in UNC5B expression (~1.5-fold, Fig. 1C). No change in UNC5A mRNA expression was observed (Fig. 1B; Ct value >30). By Western blot analysis (Fig. 1D, 1E), neogenin, UNC5A, and UNC5B were expressed by unactivated CD4+ T cells, and expression of neogenin notably increased (~3.5-fold) following activation with PHA (Fig. 1D, 1E) or anti-CD3/CD28 (not shown). Induced expression of neogenin was also evident by flow cytometry (Fig. 1F) following 48 h of mitogenic activation of CD4+ T cells. UNC5A increased in expression following mitogenic activation, but to a lesser degree than neogenin (~1.5-fold; Fig. 1D, 1E), and UNC5B expression was also induced (~2.5-fold) following activation. We failed to observe expression of DCC at the protein level (Supplemental Fig. 1B). Immunofluorescence staining of unactivated CD4+ T cells showed minimal neogenin and UNC5A and detectable levels of UNC5B expression. However, staining of neogenin and UNC5B was prominent following 48 h of activation with PHA (2.5 μg/ml, Fig. 2). Thus, both chemoattractive (neogenin) and chemorepulsive (UNC5A and UNC5B) Netrin-1 receptors are expressed by CD4+ T cells, and each receptor is modulated following cellular activation.

Netrin-1 increases the size of migratory subpopulations of activated CD4+ T cells

To next determine the effects of Netrin-1 on CD4+ T cell migration, we used a microfluidic device that allows for the quantitative analysis of bidirectional trafficking at single-cell resolution (12) (Fig. 3A). Initially, positively selected CD4+ T cells were mitogen activated (48 h) and introduced into the device and then exposed to increasing concentration gradients of Netrin-1 during an 8-h period (Fig. 3B). Their migration characteristics were compared with cells in culture media alone as a control. We found that all concentrations of Netrin-1 enhance the number of migrating T cells from 19.0 ± 5.1% (media control) to 41.9 ± 12.2, 37.5 ± 15.7, and 28.1 ± 12.6% in Netrin-1 concentrations of 0.1, 0.5, or 5 μg/ml respectively (Fig. 3B, $p < 0.05$; Supplemental Videos 1 and 2). Netrin-1 increased the number of cells migrating toward the gradient from 8.8 ± 2.9 (in media alone) to 21.5 ± 5.1% (in 0.1 μg/ml). It also increased the number of cells migrating away from the gradient from 10.2 ± 2.6 (in media alone) to 18.2 ± 7.3% (in 0.1 μg/ml Netrin-1; Fig. 3B, $p < 0.05$). Increasing the concentration of Netrin-1 did not change these bidirectional migration patterns.

We next examined the effect of Netrin-1 on the migration of CD4+ subpopulations, including $CD4^+CD25^-$ naive and $CD4^+CD25^+CD127^{dim}$ Treg subsets. Similar to pooled populations of CD4+ cells (12), we found that low numbers of $CD4^+CD25^-$ cells

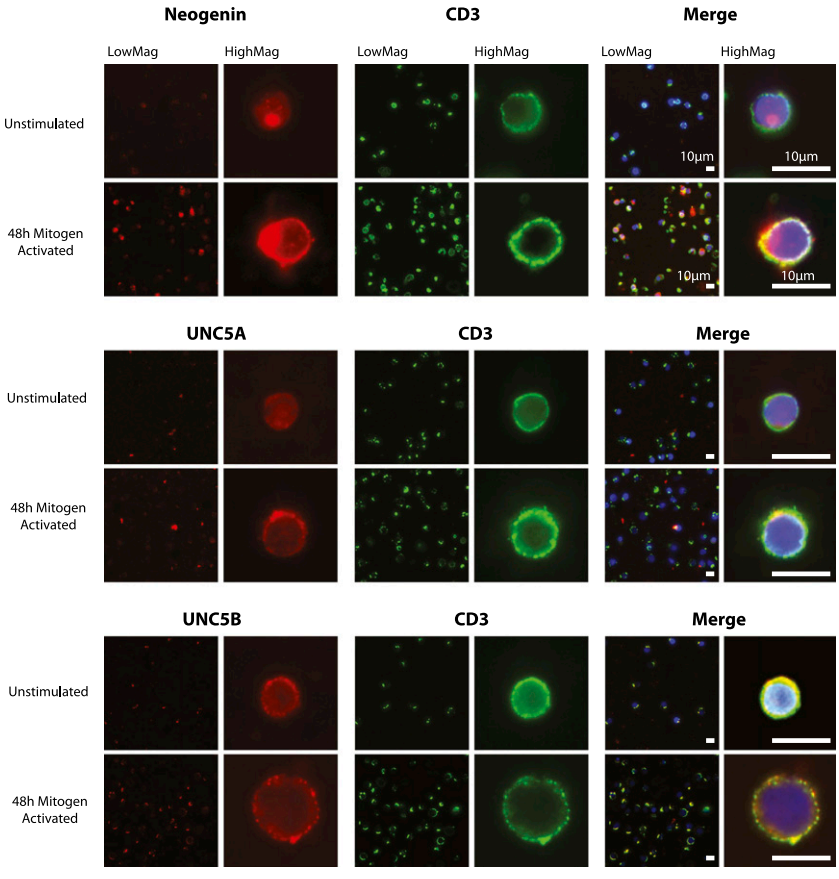

FIGURE 2. Localization of Netrin-1 receptors on CD4+ T cells. Expression of neogenin, UNC5A, and UNC5B was analyzed on unactivated or mitogen-dependent activated (PHA at 2.5 μg/ml) human CD4+ T cells by immunofluorescence staining. Netrin-1 receptor expression (red), anti-CD3 (green), and colocalization (yellow merged stain) are illustrated in the respective panels. All images are representative of $n = 3$ independent experiments.

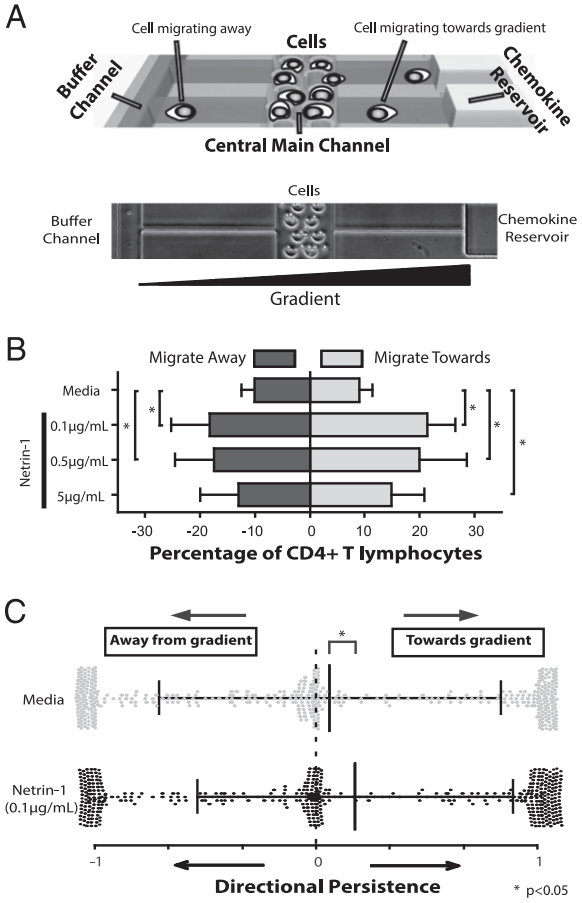

FIGURE 3. Netrin-1 increases both the size and the chemokinetic response of migrating CD4$^+$ T cells. CD4$^+$ T cell migration was analyzed in a microfluidic device that allows for the quantitative analysis of the fraction of migrating cells as well as their directionality, persistence, and speed at the single-cell level. (**A**) The microfluidic device. CD4$^+$ T cells are loaded into the central main channel and are monitored in real-time while migrating through 10-μm side channels for 8 h. Each cell has potential to migrate either toward (direction of reservoir) or away (direction of buffer channel) from a chemokine gradient. (**B**) Quantitative analysis of bidirectional migratory patterns of 48-h mitogen-activated CD4$^+$ T cells (anti-CD3/anti-CD28 at 1 μg/ml each) in response to increasing concentrations of Netrin-1, as indicated. Gray bars represent migration toward the gradient, and black bars represent migration away from the gradient (mean ± SD of $n \geq 3$ independent experiments). (**C**) Scatter plot of DP of CD4$^+$ cells in response to Netrin-1. The migratory patterns of individual CD4$^+$ T cells were evaluated and are illustrated as either gray dots (media alone) or black dots (response to Netrin-1). The black lines represent the median and SD of migratory responses under each condition. The number of cells analyzed in media alone was 449 of 2232 total migrating cells, and in Netrin-1 was 399 of 1068 total migrating cells. Illustrated are data from $n = 3$ independent experiments. *$p < 0.05$.

migrate within the device in media alone (12.3 ± 3.5%), but this subset demonstrated an induced migratory response to a Netrin-1 gradient (17.8 ± 3.0% in 0.1 μg/ml Netrin-1, Supplemental Fig. 2A). However, surprisingly few Tregs were observed to migrate within the device in media alone (7.6 ± 4.6% cells migrating), and the addition of Netrin-1 failed to increase or decrease the numbers of migrating cells (6.4 ± 3.6%) or their directional migratory pattern during an 8-h period (Supplemental Fig. 2). In general, we also observed that Tregs migrate in low numbers within the device even following mitogen-dependent activation (data not shown). Consistent with these functional observations, we also noted that Treg subsets express minimal cell surface neogenin (data not shown). Collectively, these findings suggest that Netrin-1 stimulates bidirectional migratory responses in activated CD4$^+$ T effector cells by increasing the size of migratory subpopulations.

CD4$^+$ T effector cell migration is induced by Netrin-1

We next wished to map the individual migratory trajectory of Netrin-1–responsive CD4$^+$ T cells and calculate an overall DP, as previously described (12). Using the DP algorithm, we found that Netrin-1 favors persistent migration of CD4$^+$ T cells toward the gradient (DP = 0.18 versus DP = 0.06 in media alone, $p < 0.05$, Fig. 3C). We also analyzed the migration response for every cell during the 8-h observation period (Fig. 4A–C). We found that the fraction of the total cell population that migrates within the first hour increases from ~1.5% (in media alone) to ~7% in the presence of Netrin-1 ($p < 0.05$). As shown in Fig. 4A, the effect of Netrin-1

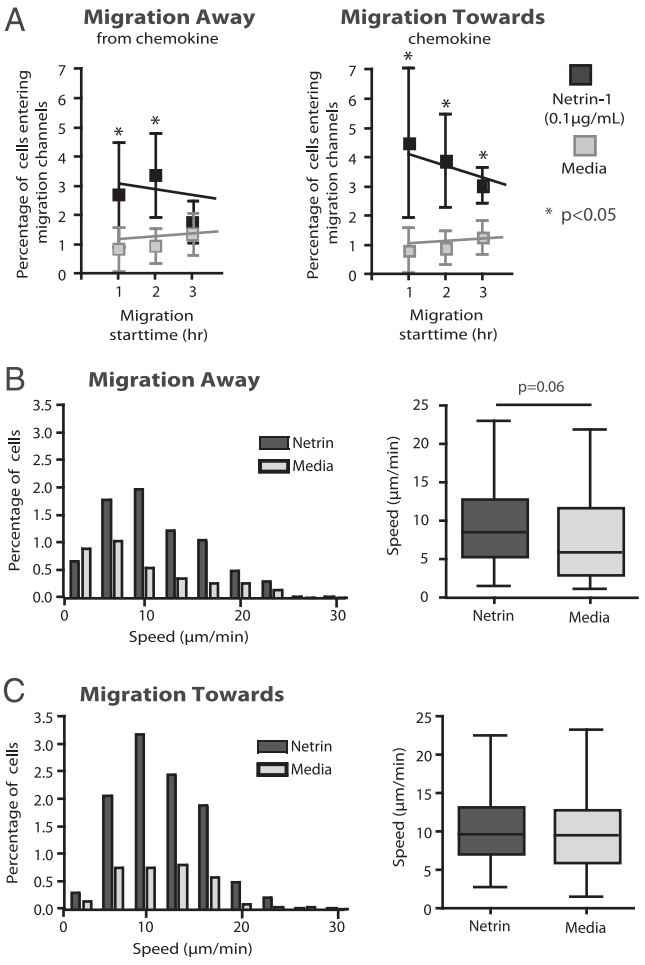

FIGURE 4. Migration characteristics of CD4$^+$ T lymphocytes in response to Netrin-1. Migration patterns of individual T cells were analyzed using time-lapse videos during an 8-h time. (**A**) Time distribution of the initial migratory response and the hourly response during the course of each experiment. The effect of Netrin-1 was prominent in the first 3 h of migration. Black symbols represent cell migration in response to Netrin-1, whereas gray symbols represent response in media alone. In (**B**) and (**C**), the percentage of cells that migrate at each indicated speed (in micrometers per minute) is separated into groups of 3.3-μm/min intervals, for cells migrating away from the gradient (B) and toward the gradient (C). Black bars represent cells migrating in response to Netrin-1, and gray bars represent cells migrating in response to media alone (as a control). The average migratory speed for each condition is shown in the box-and-whiskers plot. Error bars represent mean ± SD. The number of cells analyzed in media was 449 of 2232 total and in Netrin-1 was 399 of 1069 total. Illustrated data are from $n \geq 3$ independent experiments. *$p < 0.05$.

on the induction of migration was prominent in the first 3 h. The average speed of cells migrating in the direction of the Netrin-1 gradient did not increase (10.3 ± 4.2 μm/min) as compared with culture medium alone (9.9 ± 4.7 μm/min, Fig. 4C). The speed of migration away from the Netrin-1 gradient was also comparable to the response in media (Fig. 4B). Collectively, these findings indicate that the total fraction of migrating $CD4^+$ cells increases in the presence of Netrin-1, and that Netrin-1 favors persistent migration toward a gradient without affecting speed.

Minimal effect of Netrin-1 on RANTES-induced migration

Because our studies indicated that Netrin-1 functions to increase the size of migratory subpopulations, we postulated that it alters migration toward established chemokines. We used RANTES (100 nM) as a reference chemoattractant chemokine (29). As expected, we found that RANTES induced a marked chemoattractant response in 22.2 ± 5.0% of mitogen-activated $CD4^+$ T cells in our microfluidic device. However, when Netrin-1 (0.1 μg/ml) was combined with RANTES, the chemoattractant response did not change significantly (chemoattraction in 22.2 ± 9.5% cells, Fig. 5A). RANTES also increased migration speed versus cells in media alone (12.1 ± 5.2 μm/min versus 10.9 ± 5.2 μm/min, $p < 0.01$), and the combination of Netrin-1 with RANTES failed to change this response significantly (Fig. 5B). Thus, Netrin-1 does not enhance or inhibit the promigratory effects of the potent chemoattractant chemokine RANTES.

Netrin-1/neogenin interactions function to augment migration of $CD4^+$ T cells

Owing to its high level of expression, we next wished to determine if neogenin regulates Netrin-1 responsiveness in activated $CD4^+$ cells. To test this possibility, we infected human $CD4^+$ T cells with two different neogenin shRNA lentiviral constructs (knockdown efficiency of 50–70%, Supplemental Fig. 3) or a control shRNA, and we evaluated migration in response to Netrin-1. As illustrated in Fig. 6A, we found that the bidirectional migratory response to Netrin-1 was significantly reduced in neogenin shRNA-infected cells as compared with control shRNA-infected cells ($p < 0.05$). There was a prominent inhibitory effect on the migratory response toward Netrin-1 (11.3 ± 4.1% in controls versus 2.9 ± 1.8% in shRNA-infected cells, $p < 0.05$, Fig. 6B) as well as on the migratory response away from Netrin-1 (10.3 ± 3.4% in controls and 4.3 ± 3.7% in shRNA-infected cells, $p < 0.05$, Fig. 6B). These findings are most suggestive that neogenin functions as a promigratory/chemokinetic receptor and does not confer preferential directionality to cells within

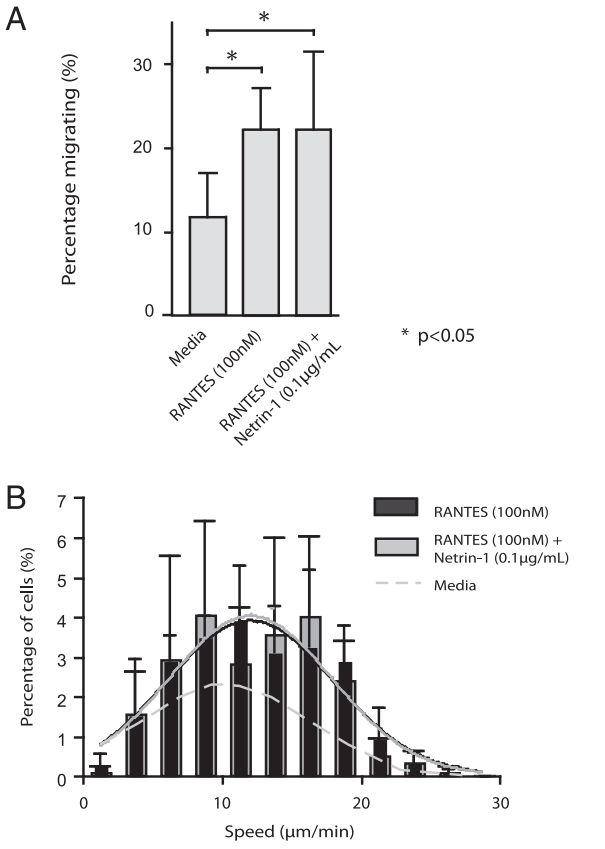

FIGURE 5. Effect of Netrin-1 on RANTES-induced migration. $CD4^+$ T cells were loaded in the microfluidic device and were exposed to a RANTES gradient in the absence or presence of Netrin-1 (0.1 μg/ml). (**A**) Percentage of cells migrating in the direction of the gradient during an 8-h period. (**B**) Migratory speed of individual T cells. The black bars represent migratory speed induced by RANTES, and the gray bars represent migration speed in response to both RANTES and Netrin-1. The dashed gray line illustrates the speed distribution in media alone. Solid gray and black lines illustrate the distribution of migratory speed for RANTES with (gray) or without (black) Netrin-1. Illustrated is the combined data from $n = 3$ independent experiments showing responses in $n = 377$ (RANTES alone) and $n = 256$ (RANTES plus Netrin-1) migrating cells. Bars represent the mean ± SD. *$p < 0.05$.

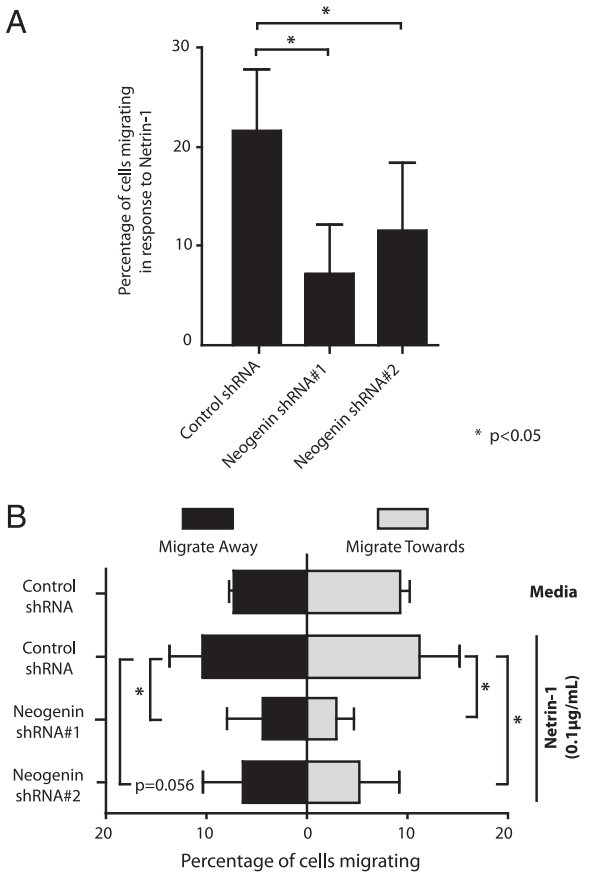

FIGURE 6. Knockdown of neogenin attenuates the migratory response to Netrin-1. Human $CD4^+$ T cells were infected with two neogenin shRNAs, each yielding a knockdown efficiency of 50–70% (as shown in Supplemental Fig. 3). Control shRNA or neogenin shRNA-infected $CD4^+$ T cells were loaded into microfluidic devices and the percentage of cells migrating in response to Netrin-1 was evaluated (**A**). In (**B**), bidirectional migratory patterns were evaluated in response to Netrin-1 (0.1 μg/ml) versus media alone using control shRNA or neogenin shRNA-infected $CD4^+$ T cells. Error bars represent mean ± SD. Data shown are from $n = 3$ independent experiments with a total of $n = 1120$ (neogenin shRNA no. 1), $n = 1324$ (neogenin shRNA no. 2), and $n = 1222$ (control shRNA) analyzed cells. *$p < 0.05$.

the Netrin-1 gradient. Furthermore, they suggest that the Netrin-1–induced migratory response is a function of random neogenin-regulated chemokinesis.

Effects of Netrin-1 on T cell activation

Previous work has shown that Netrin-1 binds the UNC family of receptors on murine $CD4^+$ T cells to inhibit cytokine production (15). Although we observed minimal expression of UNC5A/B on human $CD4^+$ T cell subsets, we also wished to determine whether Netrin-1 regulates activation responses. Freshly isolated $CD4^+$ $CD25^-$ T cells were cultured with plate-bound anti-CD3 (1 μg/ml) for 24–48 h in the absence or presence of increasing concentrations of Netrin-1 (0.1–1 μg/ml). Cytokine production (IL-2, IL-4, IL-5, IL-6, IL-10, IL-17A, and IFN-γ) was evaluated at the mRNA level. We observed a marked increase in cytokine production in anti-CD3–treated cells, but coculture with Netrin-1 failed to alter this activation response (Supplemental Fig. 4 and data not shown). Additionally, coculture of induced Tregs with Netrin-1 failed to alter the expansion of $CD4^+CD25^{hi}FOXP3^+$ T cells in vitro (data not show). Thus, Netrin-1 does not regulate mitogen-dependent activation of human $CD4^+$ T cell subsets, consistent with their low levels of expression of UNC5 family molecules.

Pathophysiological significance of Netrin-1/neogenin interactions in vivo

Next, we evaluated the effect of Netrin-1 on the recruitment of T cells into sites of inflammation in vivo. For these studies, we initially used a humanized SCID mouse model that is well established in our laboratory (30–33). In this model, human skin is allowed to engraft onto SCID mice during a 6-wk period, after which 3×10^8 human PBMCs are adoptively transferred by i.p. injection. Netrin-1 (5 μg in matrigel) was injected intradermally into the transplanted human skin on day 0 and day 7 posttransfer, and the skin was harvested on day 14 for evaluation of leukocytic infiltrates (Fig. 7A); intradermal injection of Matrigel/PBS alone served as a negative control. By H&E staining, we observed focal leukocytic infiltrates within control skins harvested from humanized mice (307 ± 58 cells per high power field (hpf), Fig. 7B). In contrast, diffuse infiltrates were present throughout skins following intradermal injection of Netrin-1 (466 ± 24 cells per hpf, Fig. 7B). Overall, by semi-quantitative grid counting there was an ~1.5-fold increase ($p < 0.01$) in infiltrates in Netrin-1–injected skins, as compared with negative control skins (Fig. 7B). By immunohistochemistry using anti-CD3, there was an ~2-fold increase in the number of T cell infiltrates in Netrin-1–injected skins versus negative controls (162 ± 59 T lymphocytes per hpf versus 86 ± 51, $p < 0.01$, Fig. 7C).

We also analyzed the expression of neogenin on $CD3^+$ T cell infiltrates within the harvested skin tissue. Interestingly, we found diffuse expression of neogenin throughout the skin grafts (Fig. 7D) on infiltrates as well as on interstitial cells and blood vessels. Using double immunofluorescence staining, we found marked colocalization of the neogenin receptor on $CD3^+$ T cells (Fig. 7D, 7E), suggesting that infiltrating neogenin-expressing T cells respond to Netrin-1 in vivo.

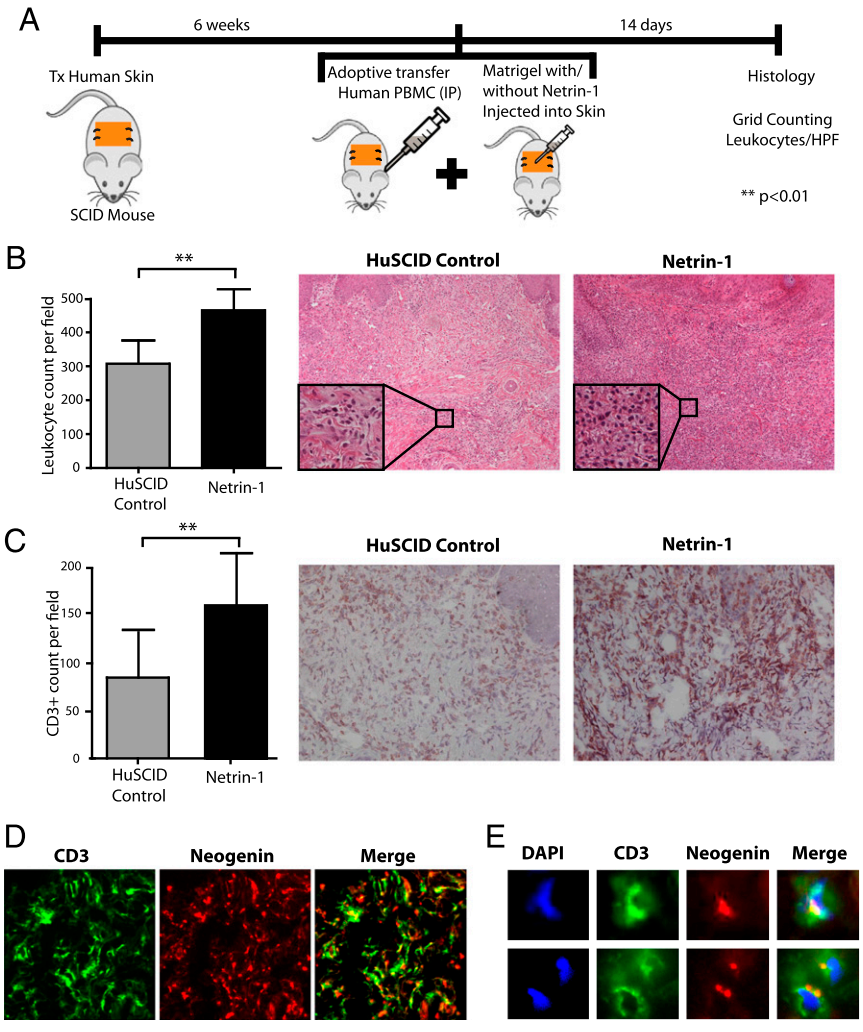

FIGURE 7. Effect of Netrin-1 on leukocyte infiltration in vivo. (**A**) Cartoon of the huSCID model; human skin is transplanted onto SCID mice, and after 6 wk the mice are humanized by i.p. injection of 3×10^8 human PBMCs. On day 0 and day 7, Netrin-1/Matrigel (5 μg) or Matrigel alone is injected s.c. into the human skin graft. (**B**) H&E staining of human skin samples harvested on day 14 after humanization. Representative histology is shown in the right panels (original magnification ×100; box inset, original magnification ×400); the average number of infiltrates in each skin was grid counted (as described in Ref. 30) and is shown in the left bar graph ($n = 8$ skins; $^{**}p < 0.01$). (**C**) Representative cryosections (original magnification ×100) from day 14 skin samples immunostained with anti-CD3; the number of $CD3^+$ T cells was grid counted and the average $CD3^+$ T cell count (mean ± SD) is illustrated in the bar graph (left panel) ($n = 8$, $^{**}p < 0.01$). (**D**) Representative immunofluorescence staining (original magnification ×100) of a Netrin-1–treated human skin graft using anti-CD3 (green stain) and anti-neogenin (red stain); colocalization is seen in the merged image as yellow color. (**E**) High original magnification (original magnification ×400) immunofluorescence images of (D), showing polarized expression of neogenin receptors on the $CD3^+$ T cell surface as the merged yellow image. Nuclei are stained with DAPI (blue).

Finally, we analyzed the colocalization of neogenin with CD3$^+$ infiltrates in human endomyocardial allograft biopsies ($n = 6$) with varying degrees of rejection. By grid counting, we found that neogenin was expressed on 12.4 ± 8.5% and 17.9 ± 10.5% of CD3$^+$ cells in biopsies either with isolated (Fig. 8A) or focal (Fig. 8B) infiltrates, respectively. We interpret these findings to suggest that the expression of neogenin on T cells is of great pathophysiological significance in vivo, and that it functions to elicit a T cell chemokinetic response in the process of T cell infiltration into human allografts.

Discussion

In this study, we show that the axonal guidance molecule Netrin-1 stimulates bidirectional migration of human CD4$^+$ T cells. Our results are based on the use of a novel microfluidic device that allows for the characterization of migration in terms of directionality, speed, and persistence at single-cell resolution. Our findings indicate that Netrin-1 increases the fraction of migrating CD4$^+$ cells and stimulates bidirectional chemokinesis, but it does not alter the directionality or the speed of the motile cells in vitro. shRNA knockdown of neogenin in human CD4$^+$ T cells has marked effects to inhibit bidirectional migration and chemokinesis, suggesting that Netrin-1/neogenin interactions elicit these migratory responses. When administered in vivo, Netrin-1 increases the local accumulation of neogenin-expressing CD3$^+$ T cell infiltrates into human skin on the huSCID mouse. Additionally, neogenin colocalizes with CD3 on infiltrates within human endomyocardial biopsies from cardiac transplant recipients. Collectively, these findings suggest that Netrin-1/neogenin interactions are pathophysiological to enhance T cell chemokinesis in association with acute inflammation and allograft rejection.

The biology of Netrin-1 is complex owing to its potential to interact with both chemoattractive and chemorepulsive receptors on activated CD4$^+$ T cells. Indeed, the reported effects of Netrin-1 in inflammation are controversial. Netrin-1 has been previously described as an anti-inflammatory guidance protein via its binding to chemorepellent UNC5B in the absence of neogenin (4, 15). This effect was reported to be mediated in part via its effects on the local infiltration of neutrophils and macrophages (16, 18, 20, 34). However, more recent studies indicate that the expression of promigratory neogenin may be critical in the functional outcome of an inflammatory response (25–27, 35, 36). For example, inflammation is reduced in neogenin knockout mice in models of peritonitis, lung injury, and ischemia/reperfusion. Thus, contrary to its reported anti-inflammatory effects, these findings support the interpretation that Netrin-1 has proinflammatory properties via interactions with distinct neogenin-expressing leukocyte subsets (25–27). Our new findings in the present study indicate that the key function of Netrin-1 on CD4$^+$ T lymphocytes is to induce chemokinesis, and that its effect on either chemoattraction or chemorepulsion are a function of random directional migration and/or additional factors.

Unlike traditional assays that define migration in a single direction, these studies have characterized migration using four quantitative parameters that include the fraction of cells responding, directionality, speed, and DP. In this manner, our results illustrate new concepts and paradigms about the biology of Netrin-1 and its associated induction of migratory responses in human T cells. Our studies demonstrate that its biological effects on CD4$^+$ T cells are multiparameter, resulting in a chemokinetic migratory response similar to C5a and IL-8 (12). Furthermore, contrary to previous reports showing that Netrin-1/UNC5A/B interactions dominate and induce chemorepulsion, we did not observe repellant migratory patterns in neogenin knockdown cells. Rather, we observed a significant decrease of the population of migrating cells, without changes in directionality, similar to the

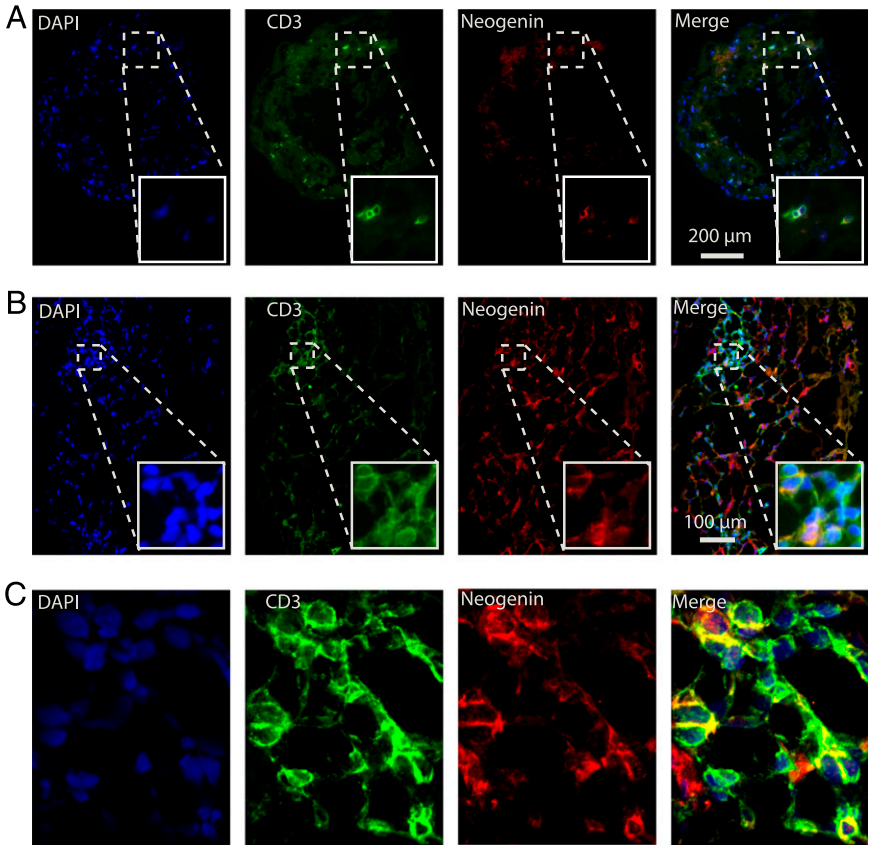

FIGURE 8. Expression of neogenin on lymphocytes within human cardiac allografts. (**A**) Immunofluorescence staining of CD3 and neogenin in a representative biopsy from a cardiac allograft with sparse CD3$^+$ T cell infiltrates. Illustrated is coexpression of neogenin with CD3 on an isolated infiltrating lymphocyte (original magnification ×100; box inset, original magnification ×200). (**B**) High-power photomicrograph of a representative biopsy showing colocalization of neogenin with CD3 within a focal infiltrate (original magnification ×200; box inset, original magnification ×400). (**C**) Confocal microscopy illustrating coexpression of CD3 and neogenin on a focal infiltrate within an allograft biopsy (original magnification ×1000).

effects of Slit2 on neutrophils (12). These new findings suggest that neuronal repellant cues inhibit leukocyte migratory activity, rather than inducing a true repellant migratory response.

Our in vitro studies indicate that Netrin-1/neogenin interactions provide a stimulus for $CD4^+$ T cell migration either toward or away from a gradient, and that directionality is dependent on the presence of additional chemoattractive or repulsive cues. However, Netrin-1 did not alter the potent chemoattractant effects of the chemokine RANTES (37–39). Thus, RANTES likely elicits a maximal signaling response resulting in chemoattraction. Overall, we interpret these data to indicate that Netrin-1/Netrin-1 receptor interactions on T cells may be independent or dependent on other cues depending on the potency of the signaling response, but that the expression of neogenin is of major biological significance in the augmentation of migratory response.

Several Netrin-1 regulated signaling pathways have potential to mediate these observed migratory responses. For example, Rho GTPases, including Rho, Rac, and Cdc42, are key elements in the control of cell shape, actin cytoskeleton reorganization, and cell motility (40). Netrin-1 activates RhoA in glioblastoma and endothelial cells, enhancing the integrity of F-actin cytoskeleton, thereby inducing cell migration and invasion (41). Rac1 and Cdc42 are also required for Netrin-1–induced axon outgrowth and neuronal cell migration during development (42, 43). Collectively, these findings are most suggestive that Netrin-1 augments Rho GTPases, which in turn elicit key migratory signals in T cells (44). Finally, Netrin-1 activates both focal adhesion kinase and Src kinase (45, 46), which may also function as key signals for chemotaxis (47). Thus, there are several Netrin-1–induced signaling responses to explain our observations and the diverse promigratory effects of T cell neogenin.

Our observations also suggest that there is some redundancy in the function of chemorepulsive UNC5 receptors on $CD4^+$ T cells. Consistent with this interpretation, medulloblastoma cells that express both neogenin and UNC5B respond to Netrin-1 with a marked migratory response resulting in increased invasiveness and angiogenesis (23). Thus, when multiple receptors are expressed by an individual cell type, high-affinity binding to neogenin may allow for a dominant activation response. In contrast, in the absence of neogenin, the binding of Netrin-1 to UNC5 family receptors alone may result in chemoinhibition. Interestingly, UNC5A/B serves as a coreceptor for neogenin, as has been described for repulsive guidance molecule-A (48). Collectively, these reports allow for the interpretation that Netrin-1/UNC5A/B interactions may be anti-inflammatory, but that these effects are redundant once Netrin-1 binds neogenin.

Finally, to translate our in vitro findings in vivo, we used an established huSCID mouse model in which it is possible to administer Netrin-1 at the local inflammatory site and test its effects on the recruitment of human lymphocytes in vivo. Based on our in vitro data, we anticipated that Netrin-1 has potential to be both proinflammatory and/or proresolution in vivo depending on the local microenvironment. However, we observed that local Netrin-1 augments lymphocyte recruitment diffusely throughout the inflammatory site, which is consistent with its observed effect of chemokinesis. Furthermore, we found abundant neogenin expression on both infiltrating lymphocytes and on other cell types, including endothelial cells. Previous work has already established that neogenin is expressed by endothelial cells, and that Netrin-1 may function as an angiogenic factor (23, 49). This allows for the interpretation that the local overexpression of Netrin-1 promotes inflammation via its direct interactions with infiltrating $CD4^+$ T cells and perhaps via indirect effects on endothelial activation. The pathophysiological importance of neogenin in T cell recruitment is further supported by our finding that it is expressed on $CD3^+$ T cells in rejecting human cardiac allografts. However, we have not excluded the possibility that these interactions may also promote chemokinesis and the emigration of lymphocytes out of tissues in the resolution phase of inflammation. Collectively, the novelty of these findings is that Netrin-1/neogenin interactions elicit bidirectional chemokinetic migration in $CD4^+$ T effectors but not in Treg subpopulations. Neogenin is expressed on activated lymphocytes in vivo in human allografts, and Netrin-1 promotes inflammation in human skin in the huSCID mouse. The translational implications of these findings is that targeting neogenin will likely have potent effects to inhibit cell-mediated immune responses, acute and chronic inflammation, and lymphocyte recruitment into allografts.

Acknowledgments

We thank Sarah Bruneau, Nora Kochupurakkal, Kaifeng Liu, and Elisabeth Wong for support with techniques and interpretation of the results of these studies. We also thank Evelyn Flynn and Josephine Koch for general help with cellular staining and immunohistochemistry and Janine van Gils and Diane Bielenberg for useful discussions. Finally, we thank Tomoshige Akino for help with quantitative PCR analysis and Nicole Mitton for editorial assistance.

Disclosures

The authors have no financial conflicts of interest.

References

1. Tessier-Lavigne, M., and C. S. Goodman. 1996. The molecular biology of axon guidance. *Science* 274: 1123–1133.
2. Klagsbrun, M., and A. Eichmann. 2005. A role for axon guidance receptors and ligands in blood vessel development and tumor angiogenesis. *Cytokine Growth Factor Rev.* 16: 535–548.
3. Gaur, P., D. R. Bielenberg, S. Samuel, D. Bose, Y. Zhou, M. J. Gray, N. A. Dallas, F. Fan, L. Xia, J. Lu, and L. M. Ellis. 2009. Role of class 3 semaphorins and their receptors in tumor growth and angiogenesis. *Clin. Cancer Res.* 15: 6763–6770. doi:10.1158/1078-0432.CCR-09-1810.
4. Ly, N. P., K. Komatsuzaki, I. P. Fraser, A. A. Tseng, P. Prodhan, K. J. Moore, and T. B. Kinane. 2005. Netrin-1 inhibits leukocyte migration in vitro and in vivo. *Proc. Natl. Acad. Sci. USA* 102: 14729–14734.
5. van Gils, J. M., M. C. Derby, L. R. Fernandes, B. Ramkhelawon, T. D. Ray, K. J. Rayner, S. Parathath, E. Distel, J. L. Feig, J. I. Alvarez-Leite, et al. 2012. The neuroimmune guidance cue netrin-1 promotes atherosclerosis by inhibiting the emigration of macrophages from plaques. *Nat. Immunol.* 13: 136–143.
6. Wu, J. Y., L. Feng, H. T. Park, N. Havlioglu, L. Wen, H. Tang, K. B. Bacon, Jiang Zh, Zhang Xc, and Y. Rao. 2001. The neuronal repellent Slit inhibits leukocyte chemotaxis induced by chemotactic factors. *Nature* 410: 948–952.
7. Takamatsu, H., and A. Kumanogoh. 2012. Diverse roles for semaphorin-plexin signaling in the immune system. *Trends Immunol.* 33: 127–135.
8. Battaglia, A., A. Buzzonetti, G. Monego, L. Peri, G. Ferrandina, F. Fanfani, G. Scambia, and A. Fattorossi. 2008. Neuropilin-1 expression identifies a subset of regulatory T cells in human lymph nodes that is modulated by preoperative chemoradiation therapy in cervical cancer. *Immunology* 123: 129–138.
9. Solomon, B. D., C. Mueller, W. J. Chae, L. M. Alabanza, and M. S. Bynoe. 2011. Neuropilin-1 attenuates autoreactivity in experimental autoimmune encephalomyelitis. *Proc. Natl. Acad. Sci. USA* 108: 2040–2045.
10. Kumanogoh, A., and H. Kikutani. 2013. Immunological functions of the neuropilins and plexins as receptors for semaphorins. *Nat. Rev. Immunol.* 13: 802–814.
11. Chaturvedi, S., D. A. Yuen, A. Bajwa, Y. W. Huang, C. Sokollik, L. Huang, G. Y. Lam, S. Tole, G. Y. Liu, J. Pan, et al. 2013. Slit2 prevents neutrophil recruitment and renal ischemia-reperfusion injury. *J. Am. Soc. Nephrol.* 24: 1274–1287.
12. Boneschansker, L., J. Yan, E. Wong, D. M. Briscoe, and D. Irimia. 2014. Microfluidic platform for the quantitative analysis of leukocyte migration signatures. *Nat. Commun.* 5: 4787.
13. Coulthard, M. G., M. Morgan, T. M. Woodruff, T. V. Arumugam, S. M. Taylor, T. C. Carpenter, M. Lackmann, and A. W. Boyd. 2012. Eph/Ephrin signaling in injury and inflammation. *Am. J. Pathol.* 181: 1493–1503.
14. Kitamura, T., Y. Kabuyama, A. Kamataki, M. K. Homma, H. Kobayashi, S. Aota, S. Kikuchi, and Y. Homma. 2008. Enhancement of lymphocyte migration and cytokine production by ephrinB1 system in rheumatoid arthritis. *Am. J. Physiol. Cell Physiol.* 294: C189–C196.
15. Tadagavadi, R. K., W. Wang, and G. Ramesh. 2010. Netrin-1 regulates Th1/Th2/Th17 cytokine production and inflammation through UNC5B receptor and protects kidney against ischemia-reperfusion injury. *J. Immunol.* 185: 3750–3758.

16. Ranganathan, P. V., C. Jayakumar, R. Mohamed, Z. Dong, and G. Ramesh. 2013. Netrin-1 regulates the inflammatory response of neutrophils and macrophages, and suppresses ischemic acute kidney injury by inhibiting COX-2-mediated PGE_2 production. *Kidney Int.* 83: 1087–1098.
17. Mehlen, P., C. Delloye-Bourgeois, and A. Chédotal. 2011. Novel roles for slits and netrins: axon guidance cues as anticancer targets? *Nat. Rev. Cancer* 11: 188–197.
18. Mirakaj, V., D. Gatidou, C. Pötzsch, K. König, and P. Rosenberger. 2011. Netrin-1 signaling dampens inflammatory peritonitis. *J. Immunol.* 186: 549–555.
19. Lai Wing Sun, K., J. P. Correia, and T. E. Kennedy. 2011. Netrins: versatile extracellular cues with diverse functions. *Development* 138: 2153–2169.
20. Mirakaj, V., C. A. Thix, S. Laucher, C. Mielke, J. C. Morote-Garcia, M. A. Schmit, J. Henes, K. E. Unertl, D. Köhler, and P. Rosenberger. 2010. Netrin-1 dampens pulmonary inflammation during acute lung injury. *Am. J. Respir. Crit. Care Med.* 181: 815–824.
21. Rosenberger, P., J. M. Schwab, V. Mirakaj, E. Masekowsky, A. Mager, J. C. Morote-Garcia, K. Unertl, and H. K. Eltzschig. 2009. Hypoxia-inducible factor-dependent induction of netrin-1 dampens inflammation caused by hypoxia. *Nat. Immunol.* 10: 195–202.
22. Aherne, C. M., C. B. Collins, J. C. Masterson, M. Tizzano, T. A. Boyle, J. A. Westrich, J. A. Parnes, G. T. Furuta, J. Rivera-Nieves, and H. K. Eltzschig. 2012. Neuronal guidance molecule netrin-1 attenuates inflammatory cell trafficking during acute experimental colitis. *Gut* 61: 695–705.
23. Akino, T., X. Han, H. Nakayama, B. McNeish, D. Zurakowski, A. Mammoto, M. Klagsbrun, and E. Smith. 2014. Netrin-1 promotes medulloblastoma cell invasiveness and angiogenesis, and demonstrates elevated expression in tumor tissue and urine of patients with pediatric medulloblastoma. *Cancer Res.* 74: 3716–3726.
24. Ramkhelawon, B., E. J. Hennessy, M. Ménager, T. D. Ray, F. J. Sheedy, S. Hutchison, A. Wanschel, S. Oldebeken, M. Geoffrion, W. Spiro, et al. 2014. Netrin-1 promotes adipose tissue macrophage retention and insulin resistance in obesity. *Nat. Med.* 20: 377–384.
25. König, K., D. Gatidou, T. Granja, J. Meier, P. Rosenberger, and V. Mirakaj. 2012. The axonal guidance receptor neogenin promotes acute inflammation. *PLoS One* 7: e32145.
26. Mirakaj, V., C. Jennewein, K. König, T. Granja, and P. Rosenberger. 2012. The guidance receptor neogenin promotes pulmonary inflammation during lung injury. *FASEB J.* 26: 1549–1558.
27. Schlegel, M., T. Granja, S. Kaiser, A. Körner, J. Henes, K. König, A. Straub, P. Rosenberger, and V. Mirakaj. 2014. Inhibition of neogenin dampens hepatic ischemia-reperfusion injury. *Crit. Care Med.* 42: e610–e619.
28. Bielenberg, D. R., A. Shimizu, and M. Klagsbrun. 2008. Semaphorin-induced cytoskeletal collapse and repulsion of endothelial cells. *Methods Enzymol.* 443: 299–314.
29. Jain, N. G., E. A. Wong, A. J. Aranyosi, L. Boneschansker, J. F. Markmann, D. M. Briscoe, and D. Irimia. 2015. Microfluidic mazes to characterize T-cell exploration patterns following activation in vitro. *Integr. Biol. (Camb.)* 7: 1423–1431.
30. Moulton, K. S., R. J. Melder, V. R. Dharnidharka, J. Hardin-Young, R. K. Jain, and D. M. Briscoe. 1999. Angiogenesis in the huPBL-SCID model of human transplant rejection. *Transplantation* 67: 1626–1631.
31. Melter, M., M. E. Reinders, M. Sho, S. Pal, C. Geehan, M. D. Denton, D. Mukhopadhyay, and D. M. Briscoe. 2000. Ligation of CD40 induces the expression of vascular endothelial growth factor by endothelial cells and monocytes and promotes angiogenesis in vivo. *Blood* 96: 3801–3808.
32. Reinders, M. E., M. Sho, A. Izawa, P. Wang, D. Mukhopadhyay, K. E. Koss, C. S. Geehan, A. D. Luster, M. H. Sayegh, and D. M. Briscoe. 2003. Proinflammatory functions of vascular endothelial growth factor in alloimmunity. *J. Clin. Invest.* 112: 1655–1665.
33. Edelbauer, M., D. Datta, I. H. Vos, A. Basu, M. P. Stack, M. E. Reinders, M. Sho, K. Calzadilla, P. Ganz, and D. M. Briscoe. 2010. Effect of vascular endothelial growth factor and its receptor KDR on the transendothelial migration and local trafficking of human T cells in vitro and in vivo. *Blood* 116: 1980–1989.
34. Chen, J., Q. P. Cai, P. J. Shen, R. L. Yan, C. M. Wang, D. J. Yang, H. B. Fu, and X. Y. Chen. 2012. Netrin-1 protects against L-arginine-induced acute pancreatitis in mice. *PLoS One* 7: e46201.
35. Mirakaj, V., S. Brown, S. Laucher, C. Steinl, G. Klein, D. Köhler, T. Skutella, C. Meisel, B. Brommer, P. Rosenberger, and J. M. Schwab. 2011. Repulsive guidance molecule-A (RGM-A) inhibits leukocyte migration and mitigates inflammation. *Proc. Natl. Acad. Sci. USA* 108: 6555–6560.
36. Muramatsu, R., T. Kubo, M. Mori, Y. Nakamura, Y. Fujita, T. Akutsu, T. Okuno, J. Taniguchi, A. Kumanogoh, M. Yoshida, et al. 2011. RGMa modulates T cell responses and is involved in autoimmune encephalomyelitis. *Nat. Med.* 17: 488–494.
37. el-Sawy, T., N. M. Fahmy, and R. L. Fairchild. 2002. Chemokines: directing leukocyte infiltration into allografts. *Curr. Opin. Immunol.* 14: 562–568.
38. Panzer, U., R. R. Reinking, O. M. Steinmetz, G. Zahner, U. Sudbeck, S. Fehr, B. Pfalzer, A. Schneider, F. Thaiss, M. Mack, et al. 2004. CXCR3 and CCR5 positive T-cell recruitment in acute human renal allograft rejection. *Transplantation* 78: 1341–1350.
39. Baggiolini, M. 1998. Chemokines and leukocyte traffic. *Nature* 392: 565–568.
40. Ridley, A. J. 2015. Rho GTPase signalling in cell migration. *Curr. Opin. Cell Biol.* 36: 103–112.
41. Shimizu, A., H. Nakayama, P. Wang, C. König, T. Akino, J. Sandlund, S. Coma, J. E. Italiano, Jr., A. Mammoto, D. R. Bielenberg, and M. Klagsbrun. 2013. Netrin-1 promotes glioblastoma cell invasiveness and angiogenesis by multiple pathways including activation of RhoA, cathepsin B, and cAMP-response element-binding protein. *J. Biol. Chem.* 288: 2210–2222.
42. Briançon-Marjollet, A., A. Ghogha, H. Nawabi, I. Triki, C. Auziol, S. Fromont, C. Piché, H. Enslen, K. Chebli, J. F. Cloutier, et al. 2008. Trio mediates netrin-1-induced Rac1 activation in axon outgrowth and guidance. *Mol. Cell. Biol.* 28: 2314–2323.
43. Causeret, F., M. Hidalgo-Sanchez, P. Fort, S. Backer, M. R. Popoff, C. Gauthier-Rouvière, and E. Bloch-Gallego. 2004. Distinct roles of Rac1/Cdc42 and Rho/Rock for axon outgrowth and nucleokinesis of precerebellar neurons toward netrin 1. *Development* 131: 2841–2852.
44. Rougerie, P., and J. Delon. 2012. Rho GTPases: masters of T lymphocyte migration and activation. *Immunol. Lett.* 142: 1–13.
45. Ren, X. R., G. L. Ming, Y. Xie, Y. Hong, D. M. Sun, Z. Q. Zhao, Z. Feng, Q. Wang, S. Shim, Z. F. Chen, et al. 2004. Focal adhesion kinase in netrin-1 signaling. *Nat. Neurosci.* 7: 1204–1212.
46. Li, W., J. Lee, H. G. Vikis, S. H. Lee, G. Liu, J. Aurandt, T. L. Shen, E. R. Fearon, J. L. Guan, M. Han, et al. 2004. Activation of FAK and Src are receptor-proximal events required for netrin signaling. *Nat. Neurosci.* 7: 1213–1221.
47. Korade-Mirnics, Z., and S. J. Corey. 2000. Src kinase-mediated signaling in leukocytes. *J. Leukoc. Biol.* 68: 603–613.
48. Hata, K., K. Kaibuchi, S. Inagaki, and T. Yamashita. 2009. Unc5B associates with LARG to mediate the action of repulsive guidance molecule. *J. Cell Biol.* 184: 737–750.
49. Park, K. W., D. Crouse, M. Lee, S. K. Karnik, L. K. Sorensen, K. J. Murphy, C. J. Kuo, and D. Y. Li. 2004. The axonal attractant Netrin-1 is an angiogenic factor. *Proc. Natl. Acad. Sci. USA* 101: 16210–16215.